

Research Article

Effect of Propolis Nanoparticles on Early-Stage Wound Healing in a Diabetic Noncontractile Wound Model

Thaís Alberti^{1*}, Daniela Coelho¹, Ana Voytena¹, Roniele Iacovski¹, Leticia Mazzarino^{1,2}, Marcelo Maraschin¹ and Beatriz Veleirinho^{1,2,3}

¹Department of Plant Science, Federal University of Santa Catarina, 88032-001 Rodovia Virgílio Várzea, Saco Grande, Florianópolis, Brazil

²NanoScoping, Solutions in Nanotechnology, 88040-400 Avenida Desembargador Vítor Lima, Trindade, Florianópolis, Brazil

³Department of Animal Science, Federal University of Santa Catarina, 88034-000, Rodovia Admar Gonzaga, 1346, Florianópolis, Brazil

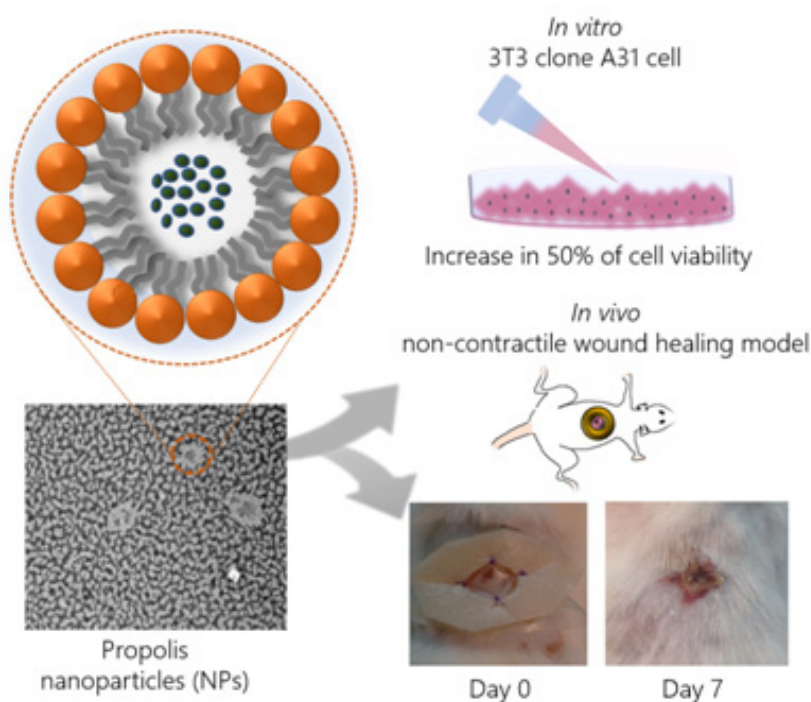
*Corresponding author: Thaís Alberti, Department of Plant Science, Federal University of Santa Catarina, 88032-001 Rodovia Virgílio Várzea, Saco Grande, Florianópolis, Brazil; E-mail: thaís.alberti@posgrad.ufsc.br

Received: March 14, 2019; Accepted: March 30, 2019; Published: April 20, 2019

Abstract

Propolis is commonly used to treat dermal inflammatory disorders and has shown great potential in experimental wound healing. However, propolis usually requires organic solvents for solubilization, which hampers its use in dermal wound healing. In this regard, nanotechnology arises as an important tool towards the development of aqueous systems with application in wound healing. In this context, the present study aimed to develop propolis nanoparticles and to evaluate, *in vitro* and *in vivo*, their potential in early-stage wound healing. Propolis Nanoparticles (PN) were characterized regarding their physical-chemical properties and chemical profile. *In vitro*, their effect on murine fibroblast cells was evaluated. *In vivo*, PN was administered in diabetic mice with impaired wound healing, using a noncontractile wound healing model. PN presented good encapsulation, stability, and phenolic content. They also stimulated growth of NIH/3T3 fibroblast cells, leading to an increase in 50% of cell viability. Mice treated with PN showed superior wound closure percentage (54.5%) when compared to untreated animals (20.7%). Taken together, our results showed that PN is promising for application in cutaneous tissue regeneration.

Graphical Abstract



Keywords: Brazilian Propolis, Nanoparticles, Wound healing, Tissue Regeneration, Diabetes mellitus.

Introduction

Over the last few decades, we have seen a worldwide increase in the use of natural products. Plants produce a great number of different metabolites which can target different molecular mechanisms simultaneously, generating synergistic therapeutic effects, even in low concentration. Phytotherapeutics also represent lower risks of toxicity and undesirable side effects compared to many synthetic molecules [1].

Propolis, also known as bee glue, is a featured natural product owing to its various biological activities and well-documented traditional use [2]. Its main pharmacological activities are antimicrobial, antitumor, antioxidant, anti-inflammatory, immunomodulatory, hypocholesterolemic, hypotensive, anesthetic, and wound healing. These activities can be linked to its chemical composition, and since the resinous mixture produced by *Apis mellifera* bees varies according to their surrounding botanical variety, the biological activity of propolis also varies [3]. Brazilian green propolis has worldwide prominence based on its abundant chemical compounds, such as prenylated phenylpropanoids, especially cinnamic acid derivatives. Among them, Artepillin C ((*E*)-3-[4-hydroxy-3, 5-bis(3-methylbut-2-enyl)phenyl]prop-2-enoic acid) has the most added value based on its antimicrobial and antitumor activities [4]. Furthermore, phenolic acids, flavonoids, mono- and sesquiterpenes have often been detected in Brazilian propolis, contributing to its chemical profile and biological activities [5]. Studies have shown that these compounds have greater antioxidant effect than commonly used antioxidants, such as vitamin C and E. By diminishing intracellular peroxides, antioxidants can also have antitumor, anti-inflammatory, and immunomodulatory activity [6]. The anti-inflammatory effect of propolis is widely documented and several studies have shown its potential in experimental wound healing.

Propolis chemical composition varies between polar and nonpolar compounds; hence, hydroalcoholic solutions have been described as the best extraction method [7]. As a result of the lipophilic characteristic of its compounds, propolis has low solubility in water, and commercial propolis formulations are often ethanol-based, which may cause adverse topical reactions. In this context, nanotechnology arises as an interesting tool that both allows the transport of lipophilic compounds in aqueous solutions and improves their stability. Nanostructured biomaterials of variable composition and with different roles in the wound healing process have been developed. These biomaterials have been extensively described as a promising alternative for the treatment of skin diseases, especially since modern wound dressing aims to create an ideal environment to provide good oxygenation, diminish bacterial colonization, and improve tissue repair [8]. In particular, nanoparticles provide properties of interest such as being nontoxic or dermal-irritating, having good physical stability, greater contact surface area, and better drug absorption [9]. Furthermore, the encapsulation of propolis into a nanoparticle system avoids the use of organic solvents which are often toxic and can harm the chemical structure of bioactive compounds. Moreover, nanoparticles may also boost the release of bioactive compounds, especially in topical use, owing to the morphology and size of the particles and their interaction with the epidermal surface.

Diabetic ulcer is one of the most worrisome conditions in the context of wound healing impairment. It is a common and serious complication of Diabetes Mellitus (DM), being one of the major causes of organ amputation which affects 15% of all diabetics. Currently, about 194 million patients living with diabetes, and WHO estimates that this number will double by 2025. The severity of wounds leads to amputation in 25% of subjects with diabetic ulcers [10]. Many studies have demonstrated that the elevation of blood glucose levels hampers resolution of the inflammatory phase and reduces angiogenesis and fibroblast proliferation, impairing the wound healing process. DM can also hinder the wound healing process by interfering with cell signaling and decreasing cell response, leading, in turn, to a reduction in peripheral blood flow and local tissue regeneration [11].

In this scenario, the present study aimed to develop Propolis Nanoparticles (PN) specific to wound healing and investigate their wound healing properties, both *in vitro* and *in vivo*. To accomplish this, a non-contractile diabetic wound healing model was previously adopted to evaluate the potential of the new formulation in individuals with compromised wound healing [12]. Aware of the limitation of using rodents, which have contractile wound healing, as opposed to human noncontractile wound healing, we adopted a model that limits wound contraction by applying silicon discs around it. This method prevents wound healing by epithelial contraction; therefore, the effect observed is by re-epithelialization and granulation, processes similar to those that occur in human tissue regeneration.

Materials and Methods

Preparation of propolis extract

A propolis sample was collected in the fall of 2015 in southern Brazil (Santa Catarina State, Sao Joaquim County, 28° 17' 38" S, 49° 55' 54" W, altitude 1353 m). Its chemical traits and low toxicity were previously determined by our research group [13]. The extraction was made using ethanol 70% (v/v) at the ratio of 0.2 mg of dried propolis per mL of solvent. The mixture was left to extract overnight at room temperature, followed by vacuum filtration to recover the hydroalcoholic extract that was further dried (1h) using a Savant™ SpeedVac™ microcentrifuge to obtain dried propolis extract.

Preparation and characterization of propolis nanoparticles

Propolis Nanoparticles (PN) were prepared using a spontaneous emulsification method with 0.4% of poloxamer (Kolliphor P188) in the aqueous phase and 2.5 mg/mL of soy lecithin in the organic phase composed of acetone and ethanol at a ratio of 60:40 (v/v). The hydroalcoholic extract was solubilized in the organic phase, reaching a final concentration in nanoparticles of 17 mg/mL after removing the organic phase in a rotary evaporator. Particle size and zeta potential were measured at 25°C by photon correlation spectroscopy, and laser Doppler anemometry, respectively, using a Zetasizer® Nano-ZS 90 (Malvern Instruments, Worcestershire, UK).

Morphology – TEM

Morphology was determined by Transmission Electronic Microscopy - TEM (CM200 Philips; FEI Company, Hillsboro, OR,

USA). Droplets of nanoparticles suspension were deposited on carbon grids and fixated with uranyl acetate 2% (w/v) following visualization.

Analysis of phenolic composition by HPLC-UV-vis

The propolis dried extract (1mg) was dissolved in ethanol and centrifuged (10 min, 4000rpm). The supernatant (0.5 mL) was collected, filtered (0.22 μm), and used for chromatographic analysis. An aliquot (60 μL , $n = 3$) was injected into a liquid chromatograph (Shimadzu LC-10A) equipped with a C18 reverse phase column (Shim-Pack CLC-ODS, 250 mm \times 4.6 mm, \emptyset 5 μm , 40°C), fitted with a C18 reversed phase guard column (Shim-Pack CLC-ODS, 4.6 mm, \emptyset 5 μm) and a UV-vis detector. Elution consisted of H_2O : AcOH: η -BuOH (350: 1: 10, v/v/v) with a flow rate at 0.8 mL/min. Identification of phenolic acids was performed using the retention times and co-chromatography of standard compounds (gallic acid, syringic acid, *p*-coumaric acid, sinapic acid, quercetin, and artemillin C – Sigma-Aldrich, MO – USA). For purposes of concentration calculations, an external standard curve was built for artemillin C under the same experimental conditions, using the integral values of the peaks' area of interest.

Encapsulation efficiency and phenolic content

Total phenolic content ($\mu\text{g/mL}$) of propolis nanoparticles was determined by the Folin-Ciocalteu spectrophotometric method [14], using a UV-vis spectrophotometer (BEL LGS 53, Monza, Italy). Analysis was carried out in triplicate, and total phenolic content was quantified using a standard curve of gallic acid ($y = 0.3344x$, $r^2 = 0.937$) in the same solvents (7.8 – 125 $\mu\text{g}\cdot\text{mL}^{-1}$). Results were expressed as mg gallic acid equivalents per g of oil (mean values \pm SD).

Encapsulation efficiency (%) was calculated using the formula described below, considering the difference between the values of total phenolic content in the PN and the nonencapsulated phenolic content, using an ultrafiltration filter device (Amicon, Ultracel-100 filter membrane, 100 kDa, Millipore Corp., USA).

Encapsulation efficiency (%) = (phenolic content of PN suspension – phenolic content of non-encapsulated fraction) \times 100/phenolic content of PN suspension.

Stability studies

To evaluate the stability of PN, samples were stored at room temperature ($25 \pm 2^\circ\text{C}$). Particle size, Polydispersity Index (PDI), zeta potential, and pH were measured after 24h and at 7, 15, 30, 60, and 90 days after preparation.

Cell Culture Studies

Murine NIH/3T3 fibroblast cells were cultivated in DMEM medium (Dulbecco's Modified Eagle's Medium) supplemented with fetal bovine serum 10% (FBS), 10 mM HEPES, 2mM L-glutamine, 100 units/mL penicillin, and 100 g/mL streptomycin. Medium was changed every 48h, and cells were maintained in culture at 37°C, humid atmosphere at 5% CO_2 . When cells were confluent, they were treated with a 0.25% (w/v) trypsin in 1mM EDTA solution and counted using a Neubauer chamber.

Cell viability essay

Toxicity of nanoparticles was determined by the neutral red uptake (NRU) assay as previously described [15]. To perform this assay, 10^4 cells/well were inoculated, and after 24h incubation at 37°C, they were treated with different concentrations of PN, blank nanoparticles, i.e., the same concentrations of nanoparticles, but without propolis, and sodium dodecyl sulfate (positive control).

After 48h incubation, the plate was washed with 100 μL PBS, stained with 100 μL of NR dye (25 $\mu\text{g/mL}$) in DMEM and incubated for another 3h. The medium containing NR was removed and washed with 100 μL PBS and 100 μL desorption solution (H_2O : EtOH: glacial acetic acid, 49: 50: 1, v/v/v). Absorbance was read in a Gold Spectrumlab 53 UV-vis Spectrophotometer (BEL Photonics, Brazil) at a wavelength of 540nm.

Wound Healing *In Vivo* Assay

Male Swiss mice (8 to 12 weeks of age) were obtained from the Central Biotery of the Federal University of Santa Catarina (Florianópolis, SC, Brazil) and housed in communal cages at $21 \pm 2^\circ\text{C}$ under a 12-h light/dark cycle (lights on at 07:00 h) with free access to food and tap water. All experimental procedures were previously approved by the Committee on the Ethical Use of Animals and performed in accordance with Brazilian regulations on animal welfare (CEUA/UFSC 23080.030926/2010-62).

Induction of experimental diabetes

Induction of experimental diabetes was performed with minor modifications of [16]. Mice were intraperitoneally injected with a single dose of streptozotocin (150mg/kg) dissolved in citrate buffer (1mM, pH 4.5). After 7 days, their blood glucose was measured with a glucometer, and mice with plasma glucose higher than 250mg/dL were considered diabetic.

Surgical procedure

Mice were anaesthetized with isoflurane and shaved; then a full-thickness round wound was made in the dorsum of the animal ($\emptyset = 0.8$ cm) using sterile scissors. In order to diminish contraction, a noncontractile wound healing model was applied as previously described by Wang et al. [26]. A strip of Tegaderm™, a transparent polyurethane dressing, was used to cover the wound.

Then, a 2mm-thick, round-auto adhesive Tegaderm™ was fixed with 4 counter lateral stitches with 5.0 nylon thread such that the wound remained at the center of the disc. The animals were randomly separated and equally distributed into four groups ($n = 6$). Mice were treated each 48h with a 100 μL treatment solution, i.e., PN, blank nanoparticles or allantoin (2.5mg/mL, positive control). The solution was injected under the Tegaderm™ and over the wound. For the negative control group, no treatment was applied. On day 7 post-surgery, animals were euthanized with an isoflurane overdose, the wounds were measured, and the wound tissues were collected for histological examination.

Histopathological analyses

Tissues were fixed in buffered formaldehyde solution (10%, v/v – pH 7.2), embedded in paraffin sections (6 μm thickness), and stained with Mallory's trichrome stain (Leica autostainer XL). Samples were scanned (Axio scan) and analyzed morphologically using the Zen software (Carl Zeiss AG, GE).

Statistical Analysis

In order to evaluate the effect of the treatments, statistical analysis was applied to the dataset, using one-way analysis of variance (ANOVA). Statistical analyses were performed using the GraphPad Prism 6 Software (GraphPad Software Inc., San Diego, CA, USA), and *p*-values less than 0.05 were considered significant. Data are presented as mean \pm SEM of independent experiments.

Results

Characterization of PN

TEM micrographs of PN produced using 0.4% poloxamer displayed a spherical shape (Figure 1). The uranyl acetate of the negative staining deposited more intensively around the nanoparticles, its higher affinity for the lecithin hydrophilic shell. The formulations showed a mean particle size similar to that obtained through photon correlation spectroscopy analysis.

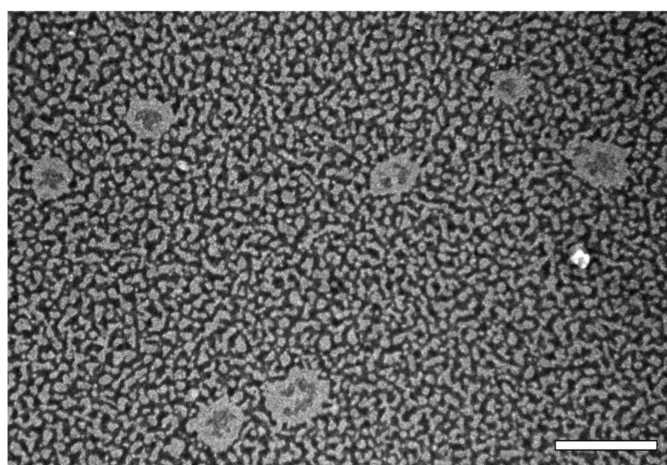


Figure 1. Transmission electron micrograph of propolis nanoparticles with 0.4% poloxamer and 2.5mg/mL of soy lecithin coating, stained with uranyl acetate at 2% (w/v). Scale bar corresponds to 0.5 μm .

Stability

Different parameters may be used for evaluating the stability of a nanoparticles-based system. Macroscopically, stability can be examined by the absence of phase separation and maintenance of the original visual characteristics. Also, the stability of physicochemical characteristics, such as size, PDI, and pH, should be evaluated [9]. Figure 2 shows the results of the average nanoparticle size at 122.1 nm. The formulation showed a unimodal distribution with a PDI of 0.126. As PDI decreases, the homogeneity of particle size increases. This value is determined by the proportion between the standard deviation and average particle size. Another important parameter is zeta potential, which measures the particle's surface electrical charge.

As this value increases, either positive or negative, generally above 30mV, electrochemical repulsion increases and, hence, stability. The negative charge of PN results from the presence of soy lecithin in the formulation, which is preferably located at the nanoparticle surface and confers a negative charge. Zeta potential remained the same throughout the evaluated time. However, after the first 7 days, a wider distribution in particle size was noted, and it remained constant until the end of the experiment, increasing PDI to a maximum of 0.253, which is within unimodal distribution. Thus, the nanoparticles presented good stability, as demonstrated by particle size and surface charge throughout the evaluated time.

Characterization of phenolic composition and encapsulation efficiency of PN

The Folin–Ciocalteu Reagent (FCR) method was used to determine the total phenolic compounds of PN (total and nonencapsulated fractions). The nonencapsulated fraction includes all compounds that were not encapsulated in the nanoparticle and that remained solubilized in aqueous phase. This fraction was separated from the intact PN, using an ultrafiltration device that retains the PN, but not the free compounds, i.e., those solubilized in aqueous phase. Encapsulation efficiency (%) represents the percentage of compounds successfully encapsulated inside the nanoparticles. The total phenolic content and encapsulation efficiency of PN are displayed in Table 1.

Table 1. Total phenolic content ($\mu\text{g}/\text{mL}$) and encapsulation efficiency (%) of PN

	Total phenolic content ($\mu\text{g}/\text{mL}$)		Encapsulation efficiency (%)
	Propolis NPs (total fraction)	Propolis NPs (non-encapsulated fraction)	
Day 0	75.31 \pm 1.05	44.77 \pm 0.75	40.55 \pm 1.34
Day 30	67.72 \pm 0.68	40.63 \pm 0.1	40.01 \pm 0.46

The average total phenolic content of PN was 75.31 $\mu\text{g}/\text{mL}$. Since the concentration of propolis extract in the nanoparticle suspension was 17 mg/mL, the average proportional concentration of phenolic compounds was 4.43 $\mu\text{g}/\text{mg}$ propolis. In turn, the concentration of nonencapsulated phenolic compounds at 44.77 $\mu\text{g}/\text{mL}$ represents about 60% of total phenolic compounds, or encapsulation efficiency of 40.55%. The encapsulation efficiency remained constant throughout the experiment.

To assess how multiple compounds from the complex matrix of propolis were distributed in the PN suspension, HPLC-UV-vis analyses of propolis extract, total fraction, and nonencapsulated fraction were performed. Representative chromatograms of propolis extract, total propolis of nanoparticles, and nonencapsulated propolis are shown in Figure 3.

The chromatographic profile of PN is similar to that of propolis extract, evidencing the presence of the six phenolic compounds identified and quantified in the extract (Table 1). Among the non-encapsulated fraction, the major compound found was gallic acid with a similar amount relative to the total PN suspension (13.7 $\mu\text{g}/\text{mL}$). On the other hand, artepillin C was detected in high

concentrations in the total PN suspension (41.9 $\mu\text{g/mL}$), but in low amounts in the nonencapsulated fraction (2.5 $\mu\text{g/mL}$). In general, a decrease in encapsulation efficiency was observed for compounds with lower retention times, i.e., more polar, such as gallic acid. This result evidences the selective encapsulation of compounds from the

propolis matrix, in which polar compounds showed a lower efficiency of encapsulation, owing to their higher affinity to the water phase, so that as compound polarity decreased, the encapsulation efficiency increased.

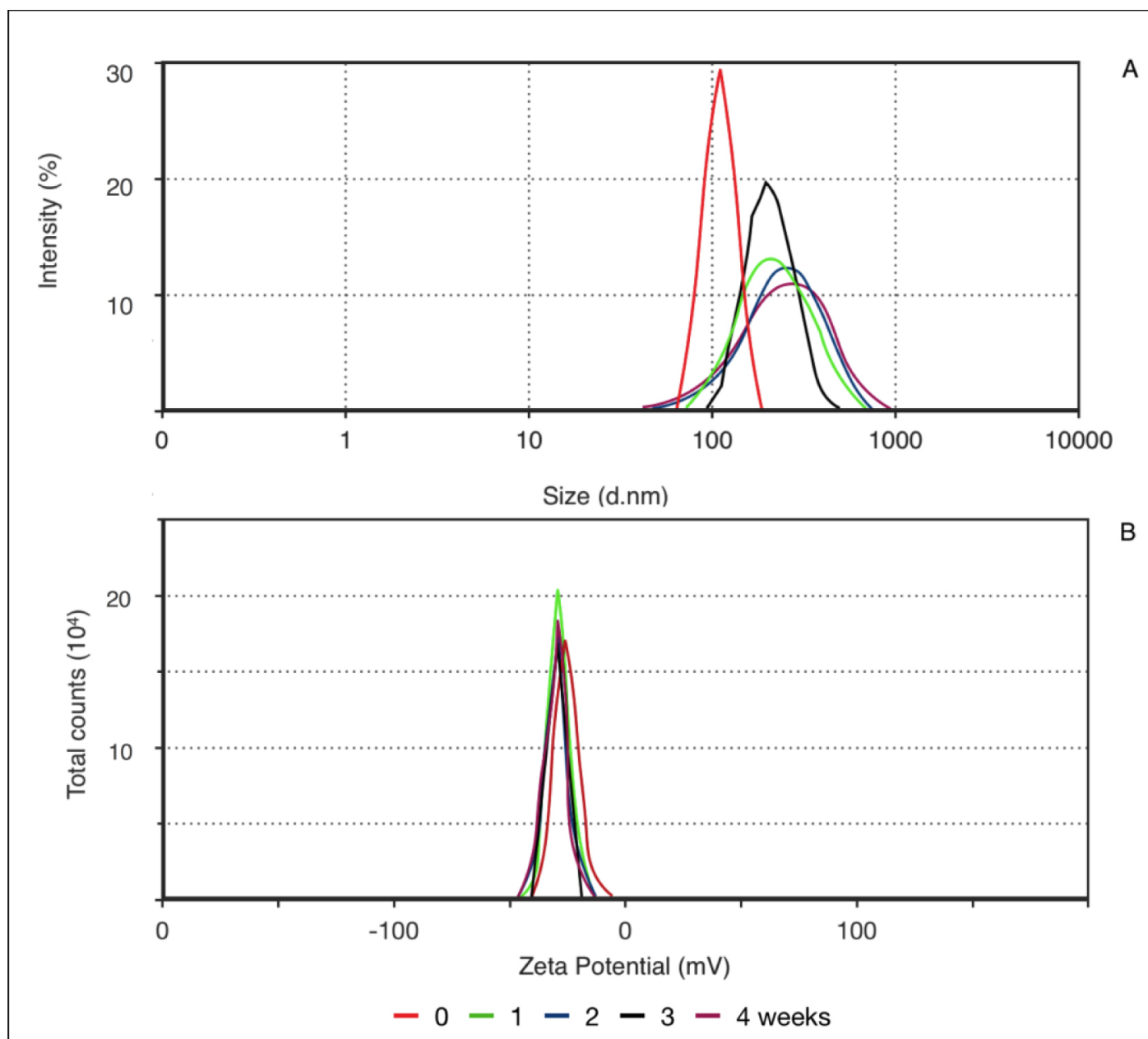


Figure 2. Correlation between mean particle size (a) and zeta potential (b) according to decay time distribution (0, 1, 2, 3, and 4 weeks).

Overall encapsulation efficiency, as shown by HPLC analysis, was 42.9%, similar to the value found by the total phenolic content assay, i.e., 40%. Moreover, total phenolic contents in PN were estimated to be 71.9 $\mu\text{g/mL}$ and 75.31 $\mu\text{g/mL}$ by chromatographic and spectrophotometric analysis, respectively. When encapsulating

a single compound, the highest possible encapsulation efficiency is desired. The nanoencapsulation of a complex mixture requires a deeper analysis accordingly to its chemical profile. HPLC analysis demonstrated that gallic acid remained in the aqueous phase. This is consistent with its chemical structure, in which 4 out of its 5 radicals

are hydroxyl groups and, therefore, highly hydrophilic with high affinity for the aqueous phase. The carboxyl group of syringic acid is also highly polar; however, the ether groups make it slightly less soluble as a result of the increasing hydrophobic nature of the alkyl chain. That explains why we could observe increasing encapsulation efficiency, but decreasing affinity, with the aqueous phase. In its turn, *p*-coumaric acid has a carboxyl group, but also an aromatic ring, making it more nonpolar than syringic acid. Sinapic acid has a chemical structure similar to that of *p*-coumaric acid, but with two more methyl ether radicals, favoring its nonpolar character. Quercetin

has 3 aromatic rings, but equally as many hydroxyls, giving it almost the same affinity to aqueous partition as that of the nonpolar fraction, explaining its 54% encapsulation efficiency. Artepillin C is a phenol constructed of single ring with two prenyl groups. Since the molecule becomes more nonpolar and therefore less soluble in water as the carbon chain becomes longer, its low molecular weight and chemical structure increase its affinity for incorporation into the phospholipidic bilayer membrane of the nanoparticle, substantiating its encapsulation efficiency by 93.9%.

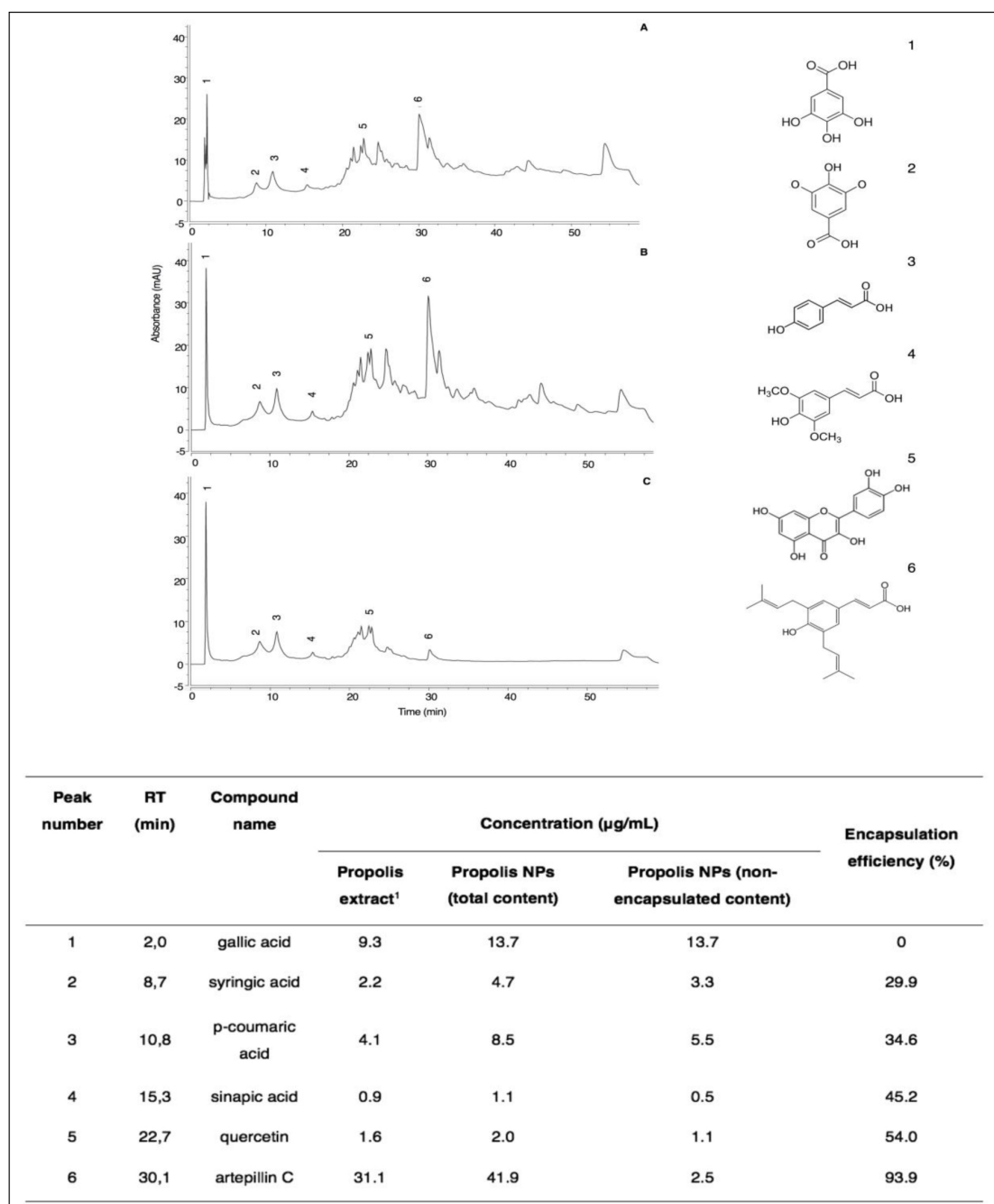


Figure 3. HPLC-UV-vis chromatograms of propolis extract (A), total content of PN (B), and free content of PN (C). Peak number 1 (gallic acid), (2) syringic acid, (3) *p*-coumaric acid, (4) sinapic acid, (5) quercetin, and (6) artepillin C. ¹ propolis concentration at 1 mg/mL.

Cell Viability Assay

The effect of PN on 3T3 fibroblasts was assessed through *in vitro* acute oral toxicity assay by measuring the neutral red uptake (NRU – Figure 4). Cells were treated with logarithmic concentrations of PN, and from the lowest concentration, i.e., 0.001 mg/mL, an increase of 50% in cell viability was observed, compared to negative control. The increase in cell viability was statistically relevant up to 0.1mg/mL, which was also the highest dosage before inhibitory concentration (IC_{50}) has been detected, showing a values of 1.30 mg/mL. The lethal dose (DL_{50}) was 1523.9 mg/kg, which corroborates previous findings described on the propolis toxicity [17].

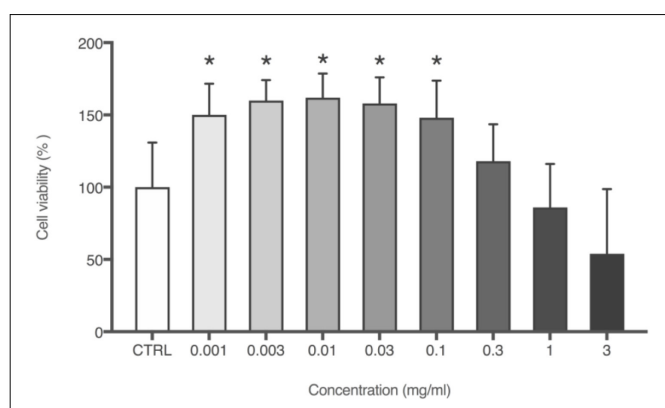


Figure 4. Cell viability (%) obtained through NRU cytotoxicity assay using 3T3 cells with logarithmic concentrations of PN (mg/mL). Each column represents the mean + SD of 6 wells/group. * $p < 0.001$ vs. control group (one-way ANOVA with Dunnett's *post-hoc* test).

Wound Healing Assay *in vivo*

Since rodents have a contractile wound healing pattern, the discs used in our noncontractile model prevented wound healing by epithelial contraction. Thus, the cicatrization effect is through re-epithelialization and granulation, processes similar to those that occur in human tissue regeneration [12]. Additionally, DM type 2 was induced to further evaluate the wound healing potential in subjects with impaired cicatrization. Mice were administered a 100 μ L treatment solution every 48h after surgical lesion. Thus, 1.7mg PN were delivered to the lesion site each treatment. Likewise, positive control (allantoin 2.5mg/mL) received 0.25mg per treatment. Figure 5 compares the percentage of wound closure area after 7 days of lesion.

All treated groups showed statistically significant wound closure percentage compared to untreated animals, which presented only 20.7% of wound closure after 7 days. PN treatment resulted in the highest percentage of wound closure (54.5%), a result quite similar to positive control (54.3%). Because of the chemical nature of PN formulation without propolis, it could be theorized that the moisture and physicochemical properties of the emulsifier present in blank nanoparticles were sufficient to positively influence the wound healing process (38.5%). Soy lecithin used as emulsifier is a phospholipid that forms phospholipid bilayers in the process of homogeneous emulsification, similar to those present in cell membranes. Nonetheless, the presence of propolis in the nanoparticles accelerated

the wound healing process by 16.0% and 33.8% in comparison to blank nanoparticles and the nontreated group, respectively.

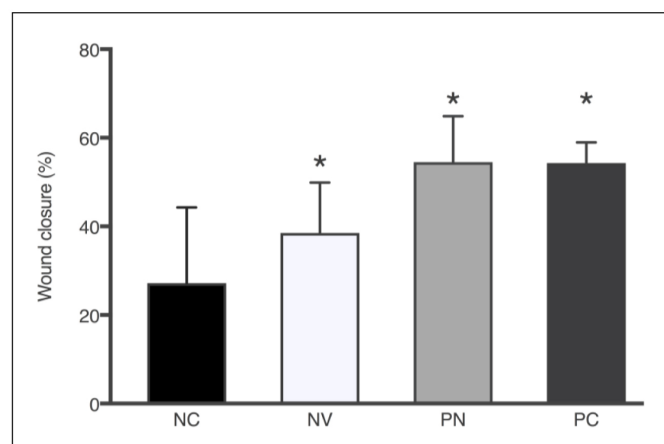


Figure 5. Wound closure area (%) after 7 days according to the treatments: NC - negative control, NV - blank nanoparticle (vehicle), PN - propolis nanoparticles, and PC - positive control. Each column represents the mean \pm SD. * $p < 0.0001$ vs. control group (one-way ANOVA with the Dunnett's *post-hoc* test).

Macroscopically, it was possible to observe changes in the aspect of the wound, as shown in Figure 6. Untreated control exhibited wound aspect of raw exposed skin, whereas blank nanoparticles (NV) seemed to have a thin layer of protective mucus. The allantoin group (PC) and PN displayed the formation of a crust typical of later stages of the wound healing process. Even though it was not the aim of our study, the results revealed an unexpected effect of PN in that some component of PN, present in both blank NV and PN, stimulated hair follicle growth. In order to perform the surgical lesion, all the animals were shaved, and all photos were taken on the same day after lesion. We were not able to observe any hair growth in untreated animals or in positive control (allantoin), only a few with random patches of fur. Interestingly, a previous study reported that propolis stimulates hair growth by inducing keratinocyte proliferation [18].

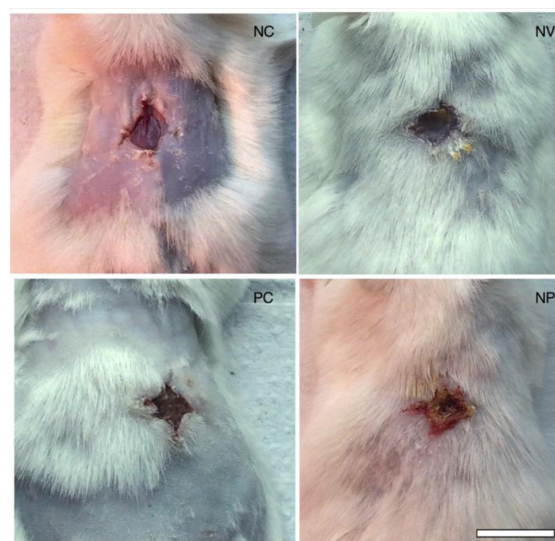


Figure 6. Photographs on day 7 post-wounding of macroscopic appearance of wounds treated with a - negative control (untreated), b - nanoparticles vehicle, c - allantoin (positive control), and d - PN. Scale bar corresponds to 1 cm and applies throughout.

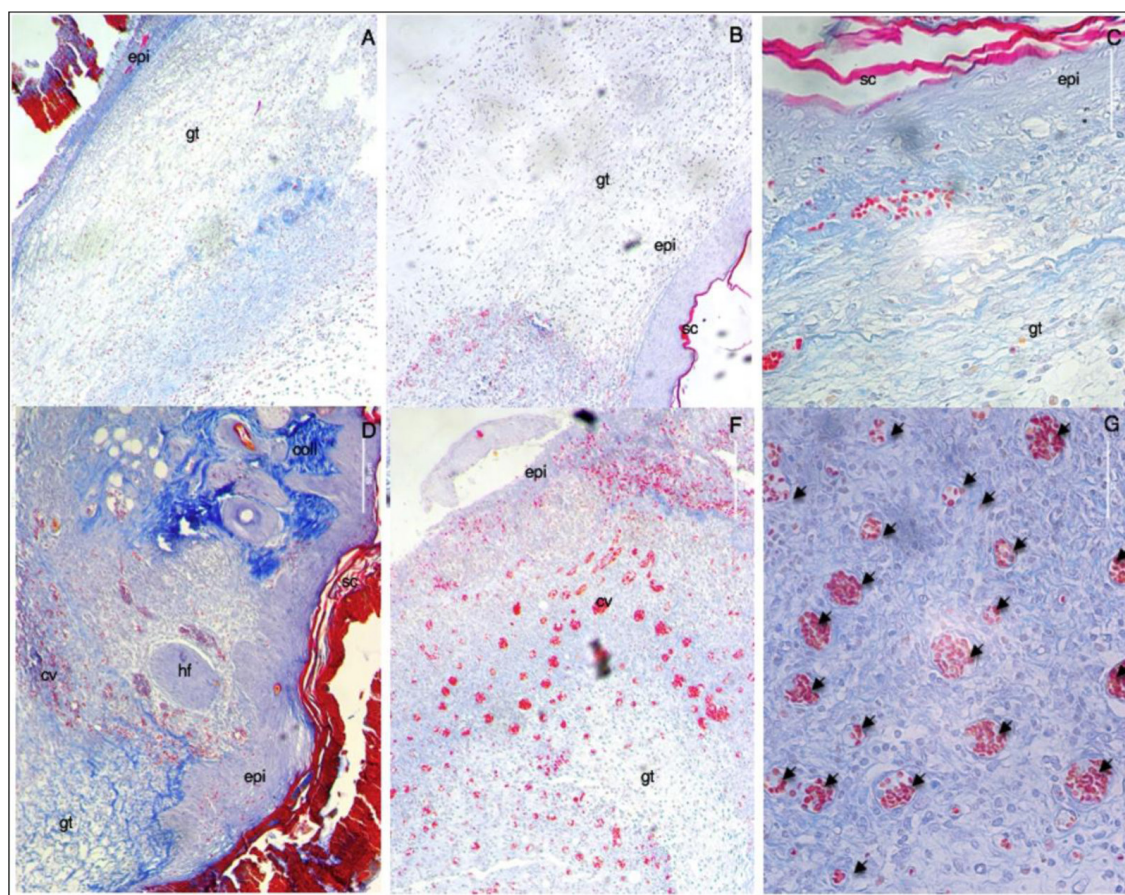


Figure 7. Representative microscopic images of the lesion region at day 7th post-wounding obtained through Mallory's staining of histological cuts. A - untreated (negative control), B - allantoin (positive control) C - nanoparticles vehicle, D - E - G propolis nanoparticles. (A-F) 10x; (G) 40x. Scale bar corresponds to 50µm and applies throughout. Abbreviations: (gt) granulation tissue; (epi) epidermis; (sc) stratum corneum; (coll) collagen; (hf) hair follicle; and capillary vases (cv and arrows).

Histological evaluation of the wound sites was performed at day 7th post-wounding, and some preliminary findings were found. On day 7 post-wounding all groups displayed formation of new epidermis, granulation tissue (high density of fibroblasts), and immature regenerated tissue (with newly synthesized unarranged collagen fibers, as detected by blue light). These data corroborate the results obtained in the macroscopic analysis of the lesions in which a similar closure was observed in the same groups. Moreover, PN showed two distinctive characteristics not found in the other groups: remodeling and angiogenesis. With the reestablishment of the functional structure of the tissue, it was possible to observe skin appendages (hair follicles), arrangement of collagen fibers resembling normal skin tissue (stained in darker blue), and numerous mature blood vessels. In the other groups, numerous red blood cells were found, but they were dispersed randomly with inflammatory infiltrates and not organized into well-defined blood vessels.

Discussion

In order to allow solubilization of nonpolar compounds in aqueous medium, propolis extract was encapsulated into a nanoparticle-based system. This system presents many advantages, such as increase in stability and compound permeation through the skin, owing to size,

morphology, and physicochemical properties of the nanoparticles and their association with the skin surface constituents. The lipophilicity of nanoparticles and the use of surfactants also increase the process of compound permeation. Nevertheless, as shown by the chemical composition analysis, propolis is a mixture of polar and nonpolar compounds with different affinities for the aqueous phase and the phospholipid bilayer of the nanoparticle. The compounds that presented medium encapsulation efficiency and, therefore, affinity with both phases may be responsible for the change in the particle size distribution noted in the first week of storage. As mentioned before, stability depends on the amount of repulsion forces between the particles, guaranteeing that they will not be attracted to each other and, thus, forming a bigger particle through coalescence. This phenomenon is known as Ostwald ripening. The zeta potential remained constant during the analyzed time. Thus, particle charge and repulsion forces were not responsible for the coalescence effect observed, which, instead, could be attributed to the polarity grade of the phenolic compounds encapsulated, such as syringic acid, *p*-coumaric acid, and sinapic acid.

The detection of a typical chemical profile associated with propolis from a specific production region or season may be used to obtain a specific pharmacological activity. The chemical fingerprint of the

propolis in the present work is consistent with the same specific harvest season and region of production as other studies determined through NMR-based metabolomics, chemometrics, machine learning algorithms [13], and UV-Vis profiles [19]. Furthermore, chromatographic profiles of the propolis herein investigated and the source of Artepillin C, the plant species *Baccharis dracunculifolia*, were similar [20]. The chromatogram highlights phenolic acids derived from benzoic acid (gallic and syringic acids) and derived from the cinamic acid (*p*-coumaric acid, sinapic acid, and ArtC), in addition to the major flavonol, quercetin. Quercetin is a flavonoid commonly found in European propolis [3] that has potent antioxidant activity and also boosts wound healing in collagen matrices [21]. Gallic acid is a potential antioxidant that directly upregulates the expression of antioxidant genes. In addition, that secondary metabolite accelerates cell migration of keratinocytes and fibroblasts in both normal and hyperglucidic conditions [23]. Syringic acid possesses both antioxidant and anti-inflammatory properties shown to protect against chemically induced inflammation [23]. Sinapic acid and its derivatives possess high radical scavenging potential which can be applied to multiple pharmacological uses [24]. In addition to antioxidant and chemoprotective properties, *p*-coumaric acid also acts as a precursor for phenylpropanoids, among them ArtC [25], the major nanoencapsulated component detected in the present study. Previous reports have shown that ArtC prevents oxidative damage in a dose-dependent manner and that it suppresses lipid peroxidation [26]. Furthermore, both Art-C and Brazilian propolis significantly inhibited alloreactive CD4 T cell proliferation and activation, as well as suppressed the expressions of IL-2, IFN- γ , and IL-17 [27]. ArtC has also been associated with propolis treatment with local and systemic anti-inflammatory activity in acute and chronic inflammation models [28].

In the present study, PN (from 0.001 mg/mL to 0.1mg/mL) presented a proliferative effect on fibroblasts, *in vitro*, increasing by 50% the cell viability. This could be associated with the accelerated wound healing effect found *in vivo*, since the proliferative phase (7 days) seems to be in a more advanced stage in comparison to the other groups such as allantoin, which macroscopically showed a similar percentage of wound closure, but did not display microscopically collagen deposition (more associated with remodeling phase), formation of skin appendages, or angiogenesis, as noted for PN. It has been shown that propolis can stimulate angiogenesis by increasing the expression of fibroblast growth factor-2 (FGF-2), a transcription factor involved in revascularization and hematopoiesis. This result was observed concomitant with fibroblast stimulation with topical application of propolis extract in the healing process of traumatic ulcer in diabetic rats [29]. FGF-2 has been found to be mediated through protein kinase (MEK/ERK) and phosphoinositide-3 kinase (PI3K/Akt) signaling pathways [30], eventually indicating a possible mechanism through which PN mediates wound healing in diabetic mice by proliferating fibroblasts, increasing collagen deposition, and forming blood capillaries and skin appendages.

Conclusion

To the best of our knowledge, this is the first report on the use of PN for wound healing. The chemical fingerprint of PN is rich

in Art C and, hence, comparable to that of green propolis, usually produced in southeastern Brazil and with claimed antitumor activity. PN stimulated fibroblast proliferation *in vitro* and induced a higher rate of wound closure *in vivo*. Likewise, our data suggest that PN induces acceleration of the proliferative phase, collagen deposition, angiogenesis, and skin appendage formation. Collectively, therefore, these results suggest that polyphenolic-rich PN has the potential to serve as a novel topical wound healing therapy in chronic wounds, including settings of impaired wound healing caused by DM.

List of Abreviation

Art C, artepillin C; PN, propolis nanoparticles; DM, diabetes mellitus; TEM, transmission electron microscopy; DMEM, dulbecco's modified eagle's medium; NRU, neutral red uptake; PDI, polydispersion index; HPLC, high performance liquid chromatography; NV, nanovehicle/blank nanoparticles; PC, positive control/allantoin group; NMR, nuclear magnetic resonance, CD4 T, T helper cells; IL-2, interleukin-2; IFN- γ , interferon gamma; IL-17, interleukin-17; FGF-2, fibroblast growth factor-2; MEK/ERK, protein kinase; PI3K/Akt, phosphoinositide-3 kinase.

Funding Information

This work was supported by CNPq, CAPES, FAPESC and PRONEX, Brazil [grant numbers 17420/2011/3, 454572/2014-0 and 401517/2012-8].

Authorship

Authors Thaís Alberti, Daniela Coelho, Ana Voytena, Roniele Iacovski, Leticia Mazzarino, Marcelo Maraschin and Beatriz Veleirinho all approved the final version of the article. The first two and last three authors contributed to the conception and design of the study. The first four authors contributed in data collection, interpretation, or analysis. The first and last two authors contributed in writing of the article and revision.

References

1. Yunes RA, Pedrosa RC, Cechinel Filho V (2001) Fármacos e fitoterápicos: a necessidade do desenvolvimento da indústria de fitoterápicos e fitofármacos no Brasil. *Química nova* 24: 147–152.
2. Ghisalberty E, Jefferies P, Lanteri R, Matsons J (1978) Constituents of propolis. *Cellular and Molecular Life Sciences*. 34:157–158.
3. Marcucci MC (1995) Propolis: chemical composition, biological properties and therapeutic activity. *Apidologie*. 26: 83–99.
4. Aga H, Shibuya T, Sugimoto T, Kurimoto M, Nakajima S (1994) Isolation and identification of antimicrobial compounds in Brazilian propolis. *Bioscience, biotechnology, and biochemistry* 58: 945–946.
5. Salatino A, Teixeira, Weinstein r, Negri G, Message D (2005) Origin and Chemical Variation of Brazilian Propolis. *Evidence-Based Complementary and Alternative Medicine* 2: 33–38.
6. Banskota AH, Tezuka Y, Kadota S (2001) Recent progress in pharmacological research of propolis. *Phytotherapy Research* 15: 561–571.
7. Park YK, Ikegaki M, Abreu JdS, Alcici NMF (1998) Estudo da preparação dos extratos de própolis e suas aplicações. *Ciência e Tecnologia de Alimentos* 18: 313–318.
8. Alberti T, S Coelho D, Voytena A, Pitz H, de Pra M, et al. (2017) Nanotechnology: A Promising Tool Towards Wound Healing. *Current pharmaceutical design*. 23: 3515–3528.
9. Tadros T, Izquierdo P, Esquena J, Solans C (2004) Formation and stability of nano-emulsions. *Adv Colloid Interface Sci* 108–109: 303–318. [crossref]

10. Gordoís A, Scuffham P, Shearer A, Oglesby A, Tobian JA (2003) The health care costs of diabetic peripheral neuropathy in the US. *Diabetes Care* 26: 1790–1795. [crossref]
11. Hehenberger K, Hansson A (1997) High glucose-induced growth factor resistance in human fibroblasts can be reversed by antioxidants and protein kinase C-inhibitors. *Cell Biochem Funct* 15: 197–201. [crossref]
12. Wang X, Ge J, Tredget EE, Wu Y (2013) The mouse excisional wound splinting model, including applications for stem cell transplantation. *Nat Protocols* 8: 302–309.
13. Maraschin M, Somensi-Zeggio AI, Oliveira SK, Kuhnen S, Tomazzoli MM, et al. (2015) Metabolic profiling and classification of propolis samples from southern Brazil: an NMR-based platform coupled with machine learning. *Journal of natural products* 79: 13–23.
14. Popova M, Bankova V, Butovska D, Petkov V, Nikolova-Damyanova B, et al. (2004) Validated methods for the quantification of biologically active constituents of poplar-type propolis. *Phytochemical analysis* 15: 235–240.
15. OECD E (2010) Guidance document on using cytotoxicity tests to estimate starting doses for acute oral systemic toxicity tests. *OECD Ser Test Assess* 20: 1–54.
16. Jain SK, Rains JL, Croad JL (2007) Effect of chromium niacinate and chromium picolinate supplementation on lipid peroxidation, TNF- α , IL-6, CRP, glycated hemoglobin, triglycerides, and cholesterol levels in blood of streptozotocin-treated diabetic rats. *Free Radical Biology and Medicine* 43: 1124–1131.
17. Park E-H, Kim S-H, Park S-S (1996) Anti-inflammatory activity of propolis. *Archives of pharmacal research* 19: 337–341.
18. Miyata S, Oda Y, Matsuo C, Kumura H, Kobayashi K (2014) Stimulatory Effect of Brazilian Propolis on Hair Growth through Proliferation of Keratinocytes in Mice. *Journal of Agricultural and Food Chemistry* 62: 11854–11861.
19. Tomazzoli MM, Neto RDP, Moresco R, Westphal L, Zeggio ARS, et al. (2015) Discrimination of Brazilian propolis according to the seasoning using chemometrics and machine learning based on UV-Vis scanning data. *Journal of integrative bioinformatics* 12:15–26.
20. Park YK, Paredes-Guzman JF, Aguiar CL, Alencar SM, Fujiwara FY (2004) Chemical constituents in *Baccharis dracunculifolia* as the main botanical origin of southeastern Brazilian propolis. *J Agric Food Chem* 52: 1100–1103. [crossref]
21. Gomathi K, Gopinath D, Rafiuddin Ahmed M, Jayakumar R (2003) Quercetin incorporated collagen matrices for dermal wound healing processes in rat. *Biomaterials* 24: 2767–2772.
22. Yang DJ, Moh SH, Son DH, You S, Kinyua AW, et al. (2016) Gallic acid promotes wound healing in normal and hyperglucidic conditions. *Molecules* 21: 899.
23. Wei X, Chen D, Yi Y, Qi H, Gao X, et al. (2012) Syringic Acid Extracted from *Herba dendrobii* Prevents Diabetic Cataract Pathogenesis by Inhibiting Aldose Reductase Activity. *Evidence-based Complementary and Alternative Medicine : eCAM* 2012: 426537.
24. Chen C (2016) Sinapic Acid and Its Derivatives as Medicine in Oxidative Stress-Induced Diseases and Aging. *Oxidative Medicine and Cellular Longevity* 2016: 10.
25. Marcucci MC, Ferreres F, García-Viguera C, Bankova VS, De Castro SL, et al. (2001) Phenolic compounds from Brazilian propolis with pharmacological activities. *J Ethnopharmacol* 74: 105–112. [crossref]
26. Shimizu K, Ashida H, Matsuura Y, Kanazawa K (2004) Antioxidative bioavailability of artepillin C in Brazilian propolis. *Arch Biochem Biophys* 424: 181–188. [crossref]
27. Cheung K-W, Sze DM-Y, Chan WK, Deng R-X, Tu W, et al. (2011) Brazilian green propolis and its constituent, Artepillin C inhibits allogeneic activated human CD4 T cells expansion and activation. *Journal of ethnopharmacology* 138: 463–471.
28. Machado JL, Assunção AKM, da Silva MCP, Reis ASD, Costa GC, et al. (2012) Brazilian green propolis: anti-inflammatory property by an immunomodulatory activity. *Evidence-Based Complementary and Alternative Medicine* 2012.
29. Puspasari A, Harijanti K, Soebadi B, Hendarti HT, Radithia D, et al. (2018) Effects of topical application of propolis extract on fibroblast growth factor-2 and fibroblast expression in the traumatic ulcers of diabetic *Rattus norvegicus*. *Journal of Oral and Maxillofacial Pathology* 22: 54.
30. Ormitz DM, Itoh N (2015) The fibroblast growth factor signaling pathway. *Wiley Interdisciplinary Reviews: Developmental Biology* 4: 215–266.

Citation:

Thaís Alberti, Daniela Coelho, Ana Voytena, Roniele Iacovski, Leticia Mazzarino, Marcelo Maraschin and Beatriz Veleirinho (2019) Effect of Propolis Nanoparticles on Early-Stage Wound Healing in a Diabetic Noncontractile Wound Model. *Nanotechnol Adv Mater Sci* Volume 2(1): 1–10.